



A Hybrid of Artificial Neural Networks and Particle Swarm Optimization Algorithm for Inverse Modeling of Leakage in Earth Dams

SeyedMahmood VaeziNejad ^{a*}, SeyedMorteza Marandi ^b, Eysa Salajegheh ^b

^a PhD Student, Civil Engineering Department, Shahid Bahonar University of Kerman, Iran.

^b Professor, Civil Engineering Department, Shahid Bahonar University of Kerman, Iran.

Received 27 May 2019; Accepted 24 July 2019

Abstract

A new intelligent hybrid method for inverse modeling (Parameter Identification) of leakage from the body and foundation of earth dams considering transient flow model has been presented in this paper. The main objective is to determine the permeability in different parts of the dams using observation data. An objective function which concurrently employs time series of hydraulic heads and flow rates observations has been defined to overcome the ill-posedness issue (nonuniqueness and instability of the identified parameters). A finite element model which considers all construction phases of an earth dam has been generated and then orthogonal design, back propagation artificial neural network and Particle Swarm Optimization algorithm has been used simultaneously to perform inverse modeling. The suggested method has been used for inverse modeling of seepage in Baft dam in Kerman, Iran as a case study. Permeability coefficients of different parts of the dam have been inspected for three distinct predefined cases and in all three cases excellent results have been attained. The highly fitting results confirm the applicability of the recommended procedure in the inverse modeling of real large-scale problems to find the origin of leakage channels which not only reduces the calculation cost but also raises the consistency and efficacy in such problems.

Keywords: Inverse Modeling; Orthogonal Design; Neural Networks; Particle Swarm Optimization Algorithm; Earth Dams.

1. Introduction

One of the most well-known bio-inspired algorithms used in optimization problems is particle swarm optimization algorithm (PSO), which basically consists of a machine-learning technique loosely inspired by birds flocking in search of food or fish schooling [1]. This algorithm is a new, computationally efficient and popular evolutionary computation algorithm that has been applied in various engineering fields such as antenna design, communication networks, clustering and classification, combinatorial optimization and specially system identification and so on in recent years [2-5].

The work of system identification (or inverse modeling) is significantly important and essential in many engineering applications, especially for system control engineering and safety analyzes. Xiang et al. [6] presented a PSO based algorithm to optimize the model parameters and simulate the nonlinear variations of the piezometric levels during the high-impact typhoons in the modeling process and raise the fitting accuracy between real piezometric levels and modeled ones. They introduced a mutation factor into the traditional piezometric level statistical model which considers the lagging effects. The suggested method was tested on Siminghu reservoir in China during typhoon Fitow and the results showed a proper agreement in the results.

* Corresponding author: vaezinejad.s.m@eng.uk.ac.ir

 <http://dx.doi.org/10.28991/cej-2019-03091392>



© 2019 by the authors. Licensee C.E.J, Tehran, Iran. This article is an open access article distributed under the terms and conditions of the Creative Commons Attribution (CC-BY) license (<http://creativecommons.org/licenses/by/4.0/>).

Chi et al. [7] suggested a method for back analysis of permeability coefficients in earth dams considering the steady state condition for seepage and tested for condition while the water level rises. The suggested method was based on the application of radial basis function neural networks (RBFNN) to minimize the mean squared error of measured and computed water heads. The PSO algorithm was used to train the RBFNN and reaching to the best structure parameters of it. The case study was done on the Nuozhadu dam in china and the attained results showed well applicability of the method.

Gamse and Oberguggenberger (2016) [8] explained the significance of different influencing terms on a rock-fill embankment dam using a statistical method on long-term coordinate time series of a geodetic point. The model was based on a hydrostatic-season-time model which was used originally for analyzing data of concrete dams. and a multiple linear regression for modeling a linear relation between observed and calculated parameters. The process of inclusion and exclusion of parameters in each direction of a predefined coordinate system and model optimizing was discussed and finally the results showed the ability of the model in abnormal leakage detection although it has its limitations.

Hydraulic conductivity (permeability) of deposits beneath the dam or in its body is one of the key factors in geotechnical structures design, which even influences their location. The main factors affecting the permeability of rocks and soils are the geometrical shape and how the gaps and available cavities are interconnected, which can be determined on site through field tests. When the obtained permeability does not precisely illustrate the status quo, uncertainties are increased, and the probability of error in the design is increased [9-12].

Past experiences designate that the layers with great permeability that were not recognized through early studies cause the water accumulation and thus the development of unusual leakage bands [13]. Also abnormal seepage phenomena may occur in earth dams due to the construction defects and material aging [14]. Zhang et al. [15], investigated the seepage field and analyzed the main causes of the abnormal seepage field in a dam with asphaltic concrete core and concluded that the main cause of the abnormal leakage might be the defect in the integrity of the anti-seepage system.

At the time of experiencing such critical phenomenon, first and foremost, the precise origin of the abnormal leakage should be detected and a review of the water-sealing system efficiency is necessary for the assessment of the leakage harmfulness and the overall stability of the dam for the decision of whether and how to treat it, because this phenomenon can cause seepage damage and lead to dam breakage. In this condition, the usage of inverse modeling concept to control dam safety by means of different instrumental readings collected continuously during its construction and operation is inevitable [7, 12, 14, 15].

The main objective of the inverse modeling is to determine the values of input parameters applied in the governing equation, such as permeability values, using the collected observations at different times and at different points within the problem domain. Typically, the monitoring points are limited in numbers, while the problem domain is continuous. Particularly, if the problem space is nonhomogeneous, the space size of the concerned parameters will be indefinite, which adds to the complexity of inverse modeling. Under the same circumstances, the use of specific methods, such as the division of the problem domain into sub-domains (where the parameter values remain constant), may be helpful [16-18].

In general, inverse modeling methods have been classified into direct and indirect categories in previous studies [18]. In the direct method, given the solution values at all points of the problem space and replacing them in the governing equation, the problem input parameters are assumed as dependent variables, and thus, a direct equation is obtained for them. In practice, the solution values are not definite at all points, and the monitoring points are distributed at limited number of points of the entire space, the readings of which are accompanied by some errors. Also, interpolation is required to obtain the solutions at the remaining points, which adds some extra errors to the problem. Therefore, the best values for input parameters are reached by incorporating the error parameter in the governing equation as well as its minimization [16, 18].

In the indirect method, the main objective is to ascertain the values of different parameters of the problem in a way that a good agreement be established between the real on-site readings and the results obtained from calculations. For this purpose, a certain objective function is introduced (e.g. the mean squared error of measured water heads and that of problem analysis by assuming a set of arbitrary input parameters) [18]. Then, the objective function is minimized using different optimization algorithms, including gradient-based search methods, genetic algorithm, particle swarm algorithm, gradual simulated annealing, etc [2, 3, 17, 19-22]. The main advantage of this method is its applicability when the number of observation points is limited. Also, it does not require the derivation of readings. However, in most of cases, we are faced with a nonlinear and non-convex optimization problem [23, 24].

Since the on-site observations of hydraulic heads are much easier and cheaper to implement than other readings, most studies on inverse modeling in leakage problems have been founded based on these parameter [17, 21, 25-27], while using only one parameter may lead to the instability or nonuniqueness of identified parameters which is called ill-posedness issue [23, 24]. An improved approach for resolving such cases is the use of more than one parameter, for example employing piezometric hydraulic heads and flow rates simultaneously, which improves the accuracy and

uniqueness of the final answer. In the other hand many previous inverse modeling studies have used the steady state model for the flow [26-28] that eases the problem complexity significantly. Unfortunately, the use of steady state model in special conditions such as permeability changing due to excavation or injection, sudden changes in the upstream pool water level or other variations occur in the model's boundary conditions, may possibly not result in accurate answers [9]. Therefore, in these cases, employing the transient flow model in the inverse analysis might be helpful [19, 22, 29].

In this research, a novel inverse modeling method has been proposed for identification of hydraulic conductivities in the problem of water leakage in earth dams. A new objective function which employs the hydraulic heads and the flow rates readings simultaneously has been applied. To improve the reliability and consistency of the solutions a transient flow model has been used in the finite element model of the problem.

Moreover the proposed method takes advantage of the orthogonal design, artificial neural networks and particle swarm optimization algorithm to decrease the calculation efforts and makes the inverse modeling of large scaled problems obtainable. The suggested method has been applied for the inverse modeling of leakage in the Baft dam located at southeast of Iran to identify the hydraulic conductivities in different parts of the dam for three different cases. The results show that the identified permeability coefficients are reasonable and properly fit the real ones, thus the proposed method provides a new mean s of accurately detecting the overall seepage behavior of earth dams while servicing.

2. Explanation of the Objective Function

If the number of permeability amounts to be governed is m , then the vector $K = [k_1, k_2, \dots, k_m]^T$ in which k_i is the permeability value in the element i is presented. Furthermore, if the number of piezometers fitted in the dam be M , then the vector $\phi_i^m = [\phi_{i1}^m, \phi_{i2}^m, \phi_{i3}^m, \dots]^T$, in which ($i = 1, 2, \dots, M$), is used to designate the hydraulic head time series in the piezometer i such that the ϕ_{it}^m is the value of hydraulic head in piezometer i at time t . Correspondingly, for N number of flowmeter, the vector $Q_j^m = [Q_{j1}^m, Q_{j2}^m, Q_{j3}^m, \dots]^T$, in which ($j = 1, 2, \dots, N$) is employed to indicate the flow rate time series in the flow meter j . In this vector, Q_{jt}^m is the flow rate measured in the flowmeter j at time t . thereupon, the objective function is defined as:

$$\min f = \left(\sum_{i=1}^M \frac{\|\phi_i(K) - \phi_i^m\|_2^2}{\|\phi_i^m\|_2^2} \right)^{\frac{1}{2}} + w \left(\sum_{j=1}^N \frac{\|Q_j(K) - Q_j^m\|_2^2}{\|Q_j^m\|_2^2} \right)^{\frac{1}{2}} \quad (1)$$

$$K_{low} \leq K \leq K_{up} \quad (2)$$

In these equations, the symbol $\|\cdot\|_2$ is using for the Euclidean norm of a vector, and $\phi_i(K)$ and $Q_j(K)$ are respectively time series related to hydraulic heads in the piezometer i and flow rates of j in the flowmeter, which outcomes from the analysis of the model with the assumption of permeability vector K . The weight parameter, w , is used to get a balance between the relative errors resulting from the error in the readings of the hydraulic heads and flow rates. K_{low} and K_{up} are the minimum and maximum of the possible permeability respectively, which could be determined through the hydrogeological characteristics of the area through field experiments.

Performing an inverse analysis in the case of large-scale geotechnical-hydrological problem does not appear to be straightforward; therefore, the present study proposed a new hybrid procedure which has benefited from orthogonal design (OD), finite element analysis (FE), artificial neural networks (ANN) and PSO algorithms. The following subsections briefly describe each of the method components.

2.1. Orthogonal Design Selection Method

The orthogonal design (OD) selection method is a very useful statistical method in which orthogonal arrays are used to design multi-factor experiments [30]. In the present study, this method have been used in the selection of different permeability compositions, $\mathbb{K} = \{K_1, K_2, K_3, \dots\}$, in such a way that not only the number of states reduce to the extent possible but also the determined compositions cover all the possible states perfectly. Each permeability composition has been used as input parameters of the leakage problem. As a result of using orthogonal design selection method, the number of necessary direct analyses and consequently the computational cost in the inverse modeling problem will reduce severely. For example, if the number of elements of the inverse problem be 6 and the number of different states of permeability for each element be 7, a full inverse analysis, using all possible responses, needs to perform finite element analysis of the problem $7^6(117649)$ times while the application of the orthogonal design method reduces the number of analysis to 49.

2.2. Finite Element Analysis

The finite element model of the problem is fully implemented in the ABAQUS software considering all construction and operation steps of the dam. This model perfectly considers non-linear effects related to the location of the lake water

level and its temporal changes, both at construction time and at the time of impounding and operation. In addition, it obtains the total heads and flow rates time series at all points in the body and foundation of the dam including the locations of instruments, namely the vectors $\phi_i(K)$ ($i = 1, 2, \dots, M$) and $Q_j(K)$ ($i = 1, 2, \dots, N$) in Equation 1.

Thereafter for each combination K_i in the space \mathbb{K} , which is determined by the orthogonal design method, the simulated problem has been performed once and the obtained results has been used to train an artificial neural network, by which the time series of response values can be obtained at each point for any desired permeability state.

2.3. Back Propagation Neural Network (BPNN)

Currently artificial neural networks are recognized as an effective way of estimating and predicting the response in non-linear multi-parameter problems. These networks, which are based on the training through educational data, are widely used in solving hydrological problems [17, 26, 31].

Among various types of artificial neural networks, back propagation neural networks can be referred to which had the highest application in the past [32].

In the present study, a back-propagation neural network has been employed as an implicit mapping between the input parameters space and the space of responses at observation points. Figure 1 illustrates the general schema of a back-propagation neural network in which there is an input layer, two hidden layers and an output layer. The number of neurons in the input layer (I) is determined by the number of input parameters, which are herein the size of K (m). The number of output layer neurons (O) also depends on the number of reading points ($M + N$). The number of neurons in the intermediate hidden layers (HI, HII) that determine the main structure of the neural network and will have the most significant effect on the training method and overall performance of the network is determined through minimizing a predefined error function on the training data by trial and errors.

In order to achieve the input data set of training data, different permeability combinations, which are determined by the orthogonal design method, are used. The output data set of the training data is provided using information of the finite element analysis at observation points.

As shown in Figure 1, in the network training, the data are first released forward (solid lines), then the error values are calculated and returned backward, and therefore the weight values at the connection points are corrected and updated (dotted lines). Here, the sigmoid transfer function is used as the transfer function, and thus all the training data are mapped linearly to the interval (0.1-0.9) before being placed in the input layer [33]. After that the Levenberg-Marquardt learning algorithm is used in the back propagation network for the training [34].

2.4. PSO Algorithm

Particle Swarm Optimization was first introduced by Dr. Russell C. Eberhart 1 and Dr. James Kennedy 2 in 1995. As described by Eberhart and Kennedy, the PSO algorithm is an adaptive algorithm based on a social-psychological metaphor; a population of individuals (referred to as particles) adapts by returning stochastically toward previously successful regions. Particle Swarm has two primary operators: Velocity update and Position update. During each generation each particle is accelerated toward the particles previous best position and the global best position. At each step a new velocity value for each particle is calculated based on its current velocity, the distance from its previous best position, and the distance from the global best position. The new velocity value is then used to calculate the next position of the particle in the search space. This process is then iterated a set number of times or until a minimum error is achieved.

PSO algorithm, which has been used greatly in the past as an optimization method, has been used widely to solve many hydrological problems related to groundwater or surface water [20-22, 35]. Here the PSO algorithm is used to find the best permeability combination through which the objective function introduced in Equation 1 is absolutely minimized, and as a result, the best compatibility is achieved between the readings of instruments and the responses obtained from the neural network. To do this, a primitive population is first created randomly, each member of the population being a state of permeability combinations in different elements, and then the operators of the PSO algorithm are performed sequentially.

3. Introducing the Characteristics of Baft Earth Dam

3.1. Specifications of Baft Dam Site

The Baft earth dam with clayey core is constructed on the Baft River, one of the branches of the Dahouj River, 160 km off the southwest of Kerman city in Kerman province to supply drinking water for Baft and Bezenjan and to control the floods of the river. Figure 2 illustrates an image of the overall view of the dam and its geographical location.

The dam catchment area is 259 km² and the volume of the reservoir lake at normal level of 2352.75 m from the sea level is 40 million m³. The dam crest length is 1160 m and its width is 10 m. the dam height is 65 m from the base, and

its base width is 227 m in the largest cross-section. It is located at latitude 29°15'30"N and at longitude 56°37'50"E in the Jazmurian watershed. General plan of the dam and its position are displayed in Figure 3.

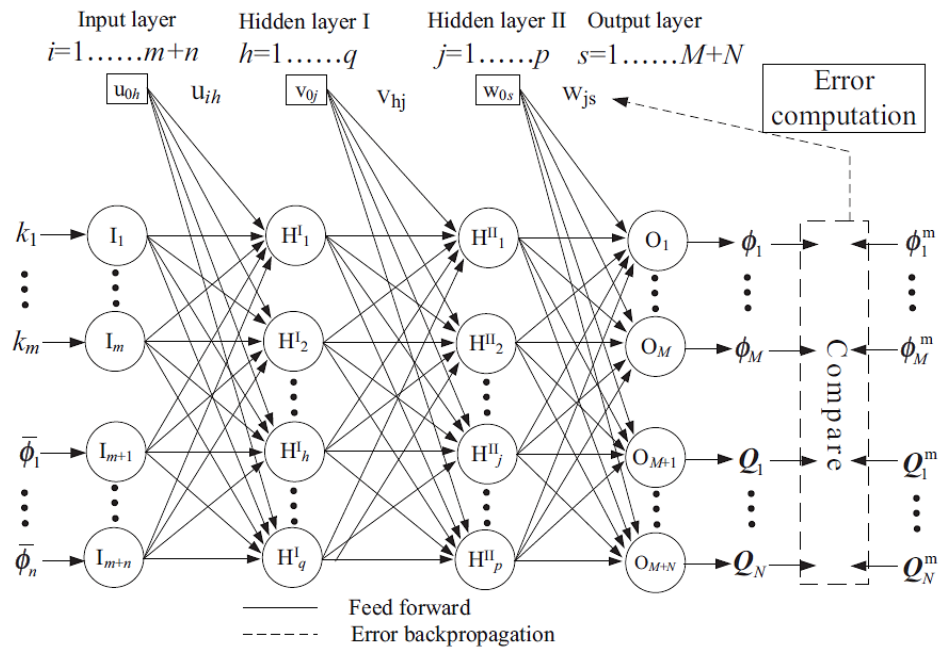


Figure 1. General schema of a two hidden-layer artificial neural network



Figure2. General view of the dam and its location

As shown in Figure 3, the river direction in the dam body is north-south and the axis of the dam is located ahead of the strait of the river, in a section with a direction of 195 degrees. The main composition of the dam site includes five different parts; the characteristics of them from the right hand side to the left hand side are as follows:

- A. The Right hand side bearing on limestone outcropping with a slope of 30 degrees and level of 2,440 meters above the sea level.
- B. The smooth right-hand slope of 210 meters in length, including surface dirt and weathered deposits with a thickness of 3 meters; in this part, the dam body after excavating the surface layers is placed on the lower blend.
- C. The middle part including flood deposits with a thickness of approximately 10 m, the width of the river in this part is 4 meters and the floor of the river is at a distance of 2,295 meters from the sea level.

- D. The limestone section that is thin at first and then its thickness increases, with a length of 335 m below the dam body.
- E. The left arm is made up of alluvial deposits with a thickness of 2 to 6 meters. The lowest point of that is 25 meters below the dam crest and its length is 380 meters.

Generally, the bottom composition of the dam axis is made of alluvial deposits. These rocks are tremendously strong and hard with a compressive strength above 150MP provided that they are not altered and weathered. However, these rocks are altered and weathered in the area beneath the dam. The permeability of these rocks is substantially low or they are even impermeable, and thus, they are very useful for the dam reservoir and foundation. Generally, for seepage sealing of the zone beneath the dam, alluvial deposits should be removed and weathered layers must be reinforced. Figure 4 depicts the typical cross-section of dam body along with different parts.

As it can be seen in the Figure 4, the clay core is in the central part and the fine-grained and coarse-grained filters surrounded it on the sides, followed by the shell layers. To protect the shell, the rock fill layer has been applied over it with a riprap layer on its upstream part. Moreover, there is a plastic concrete grout curtain in the weathered layer beneath the dam. Figure 5 shows the longitudinal profile of the dam embankment and indicates how the sealing curtain is applied along the dam. Table 1 summarizes the specifications of the different parts of the dam used in its modeling. All specifications are derived from the results of the preliminary studies and design reports. The construction operation began after the completion of the preliminary studies in August 2003 and ended in September 2010. Dam impounding began in December 2008, and until May 2009, the level of water in the reservoir has risen to the level of 2318.97 meters. However, since June 2009, a portion of this water has been released for agricultural usages and until October 2009 the level of the reservoir water has descend to 2314.68 meters. Repeatedly, by the start of the wet season in 2009, the level of water began to increase and eventually the water level in 2013 reached the level of 2352.75.

3.2. Characteristics of the Instrumentation and Measurement Systems

Continuous performance inspection of the dams, especially earthen dams, is important not only for recognizing the behavior of different parts of the dam, but also from the safety point of view and eliminating of possible defects that may lead to dam failure. Figure 6 displays different sections of the instrument implementations in the Baft dam where the modeling section of this study is shown as section G-G. Measurement tools include different kinds of piezometers, pressure gauges, seismometers, inclinometers, accelerometers, flowmeters, etc. The exact location and alignment of their installation in section G-G are shown in Figure 7.

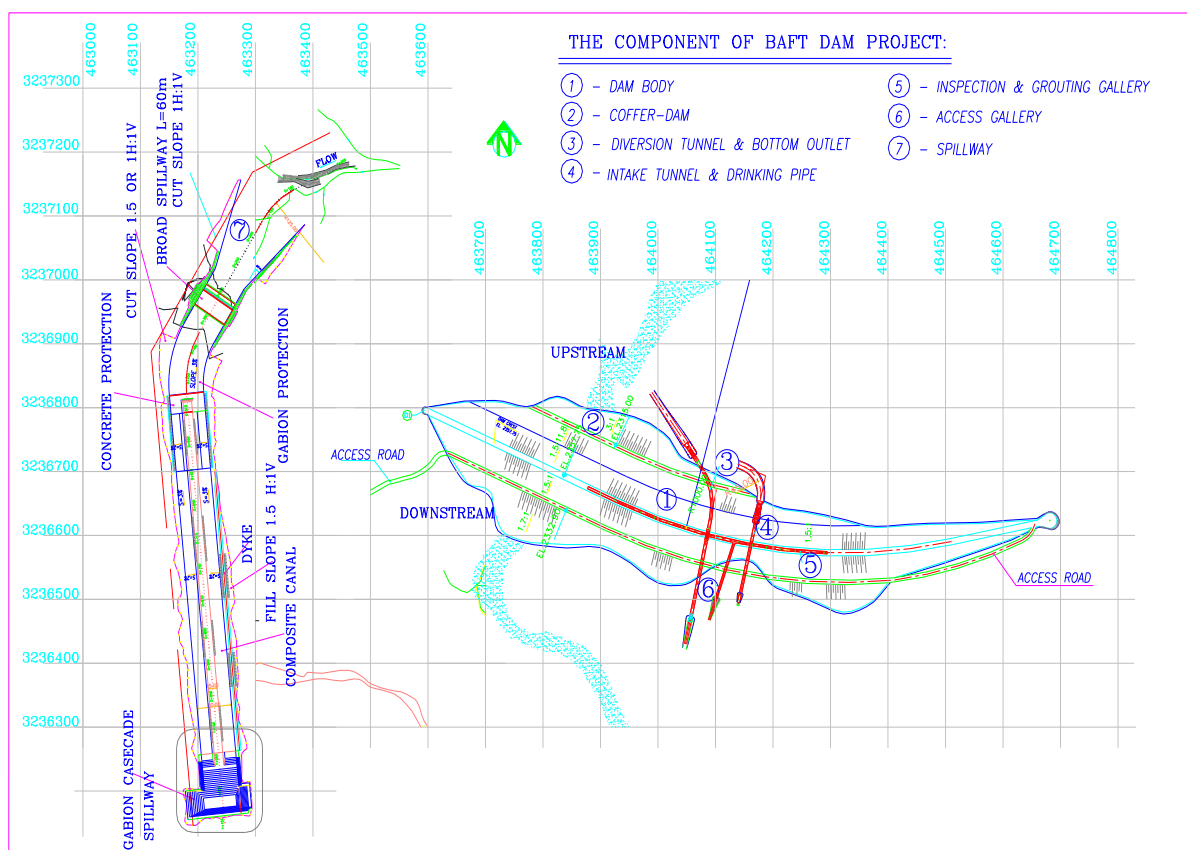


Figure 3. General plan of the dam body

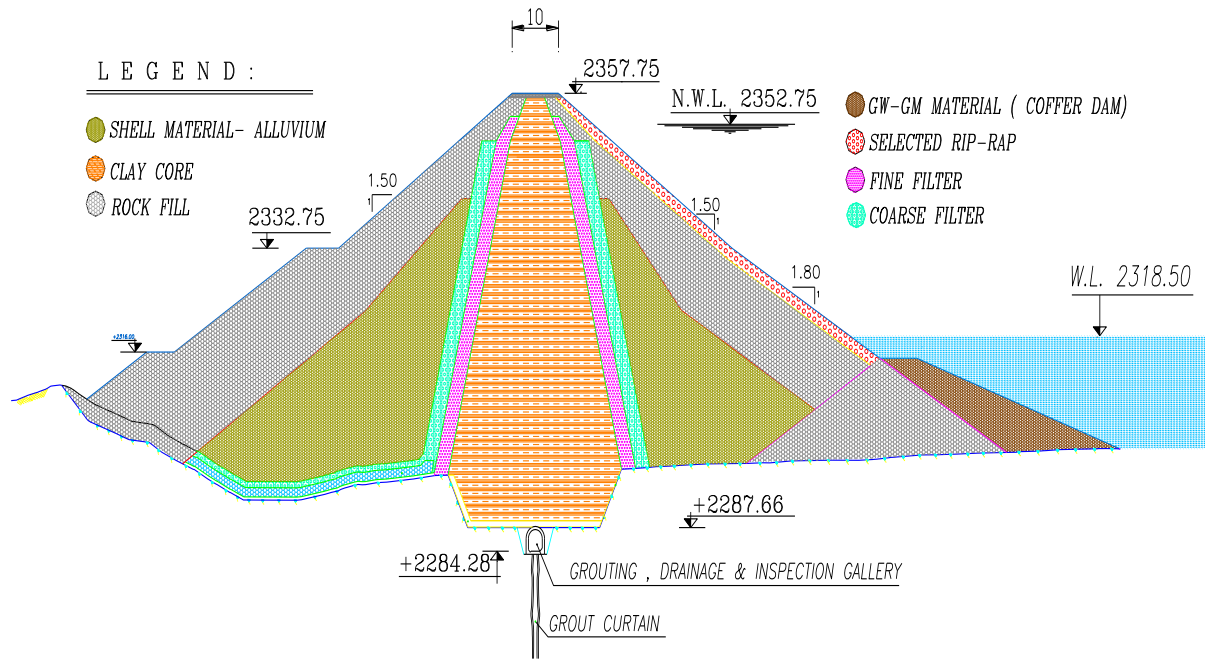


Figure 4. General section of Baft earth dam

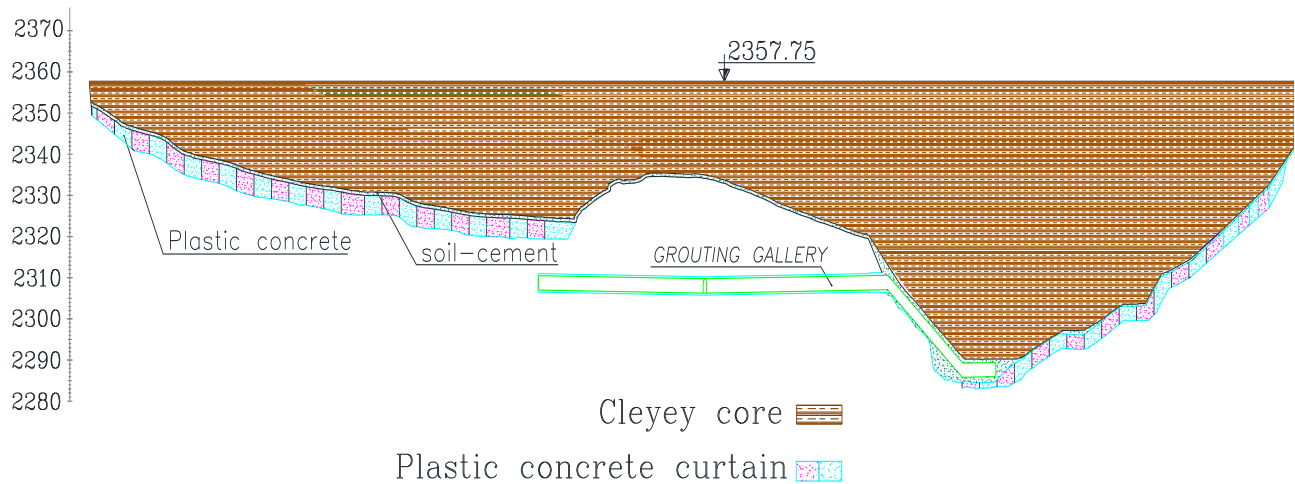


Figure 5. Longitudinal profile of the Baft earth dam

Table 1. Specifications of different parts of the dam body

	Density (kg/m ³)	Yong's modulus (MN/m ²)	Permeability in x direction (m/s)	Permeability in y direction (m/s)	cohesion (kN/m ³)	Friction Angle (degree)
Foundation	2300	500	1×10^{-7}	1×10^{-7}	250	21
Core	1900	10.75	3×10^{-8}	6×10^{-9}	80	18
Filters	1900	37	1×10^{-5}	1×10^{-5}	7	37
Shell	1900	10	1×10^{-3}	1×10^{-3}	3	45

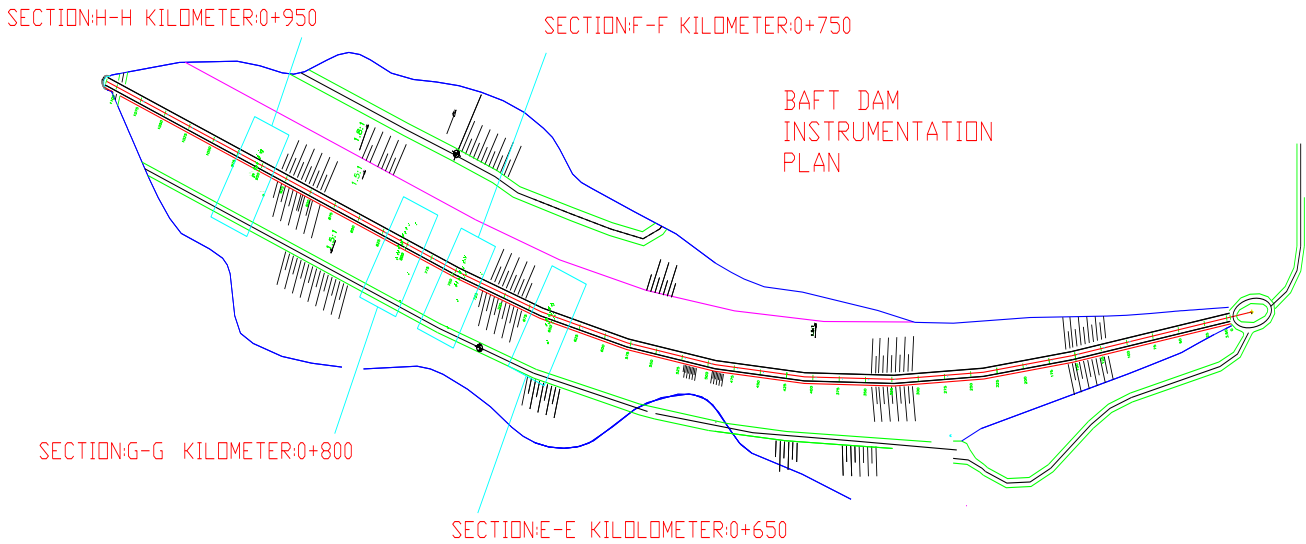


Figure 6. plan of dam body sections

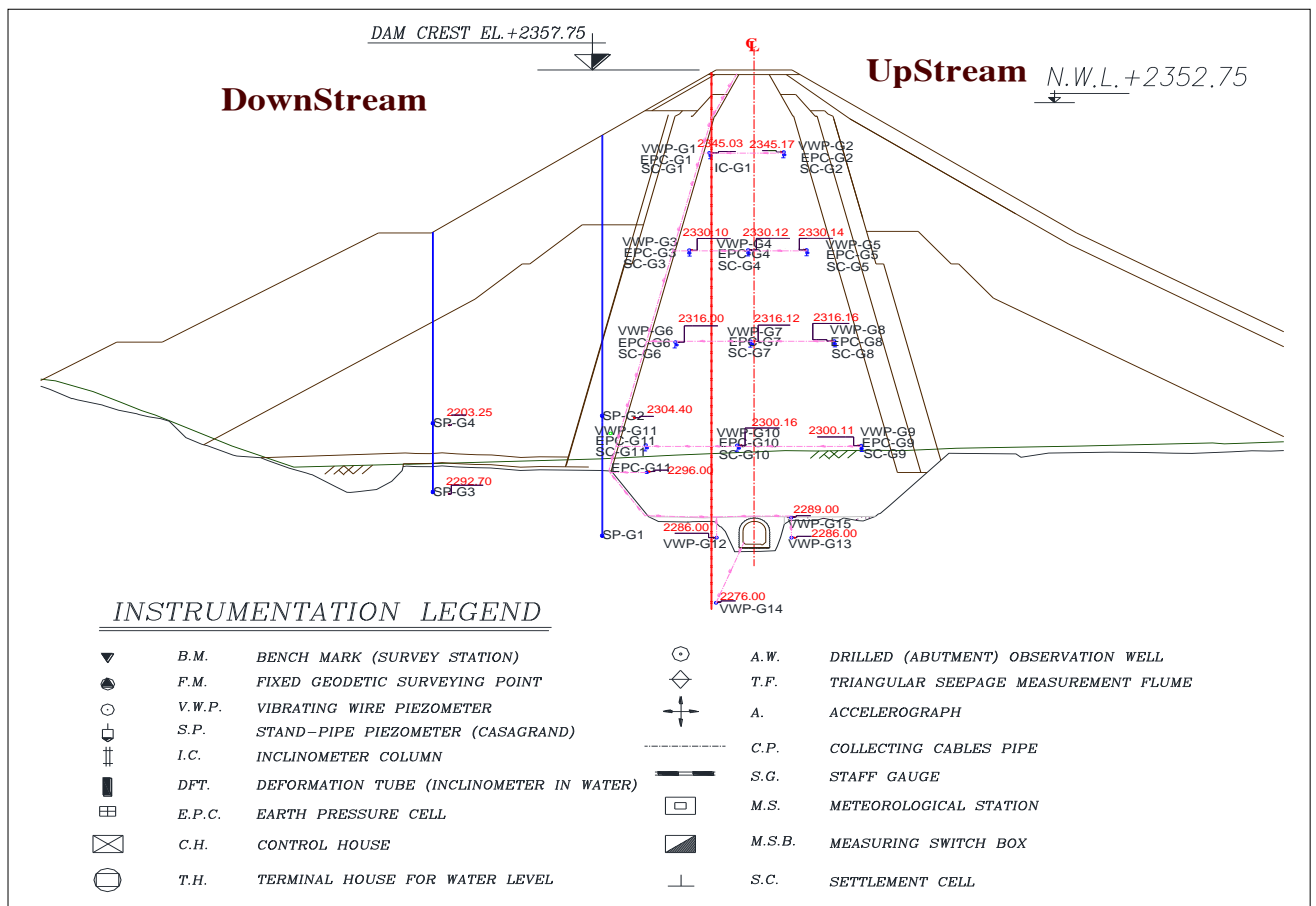


Figure 7. Instrumentation in section G-G

4. Inverse Modeling of Leakage in the Baft Earth Dam

4.1. Computational Model Structure

As previously mentioned, a finite element model was made for the seepage inverse modeling in the G-G section of the Baft dam whose location is shown in Figure 6. The constructed model consisted of 1336 6-node triangular elements and 2781 nodes. All stages of the dam construction including its needed excavation step, 21 steps of its embanking, impounding stage, consolidation and servicing stage have been modeled with regard to the actual time intervals based on the dam's factual reports. Figure 8 shows the model in the ABAQUS software at two different stages, one at the time

of body embanking and the other at the start of impounding stage. The variation of water level in the dam reservoir lake is shown in Figure 9, the impounding time intervals are actually considered in the modeling after the completion of the construction process for the aim of reality. A porous- elastic model has been used for modeling of materials behavior which has used the Mohr-Coulomb plasticity model for failure criteria in accordance with the dam designing manual.

After completion of the modeling and in order to validate the results the stability of the dam has been controlled and then the pore water pressures obtained in some particular points were compared with actual values of the piezometers readings. Figure 10 shows such comparison for the three vibrating wire piezometers G8, G10, and G12, whose exact positions are displayed in Figure 7. The reliable compatibility between the results obtained from the finite elements model and the actual results in different parts of the dam, whether in its body or in its foundation, indicates the suitability of the model for the use in reverse analysis.

4.2. Defining the Variables Space

The first step in the inverse modeling process is to determine inconsistent specifications of the model which can affect the leakage problem. Behavior controls and analyzes carried out during construction, impounding and operation of the Baft earth dam are all indicative of its proper performance and its accurate design. However, in order to evaluate the applicability of the proposed method in the inverse modeling, the permeability coefficients in a group of elements has been conceptually changed and then by assuming that the amount and exact location of these elements are unknown, based on the results of finite elements model (here hydraulic heads in a definite number of nodes and total flow discharge rates) the amount and location of the damaged elements has been searched. The general flowchart of the proposed method used in this study is as displayed in Figure 11.

For a better assessment, regarding the data from preliminary tests and studies that were available in its design reports, for each part of the dam a range for permeability value changes has been defined. Also some different compositions have been defined for the dam leakage analysis through orthogonal design method. Table 2 displays upper and lower limits of permeability changes in different parts of the dam model.

As shown in Table 2, in view of the fact that permeability in the clayey core is very small, the amount of permeability in both directions of it has been considered equal. In addition, with regard to the permeability variation intervals in different parts of the dam, seven permeability levels have been considered for each part as shown in Table 3. These permeability levels have been applied in the creation of an orthogonal design table L49 (7⁶). Consequently, a set of 49 different permeability combinations have been made to be run in the finite elements model. In favor of increasing the efficiency and accuracy of the model the foundation part has been divided into three layers as shown in Table 3.

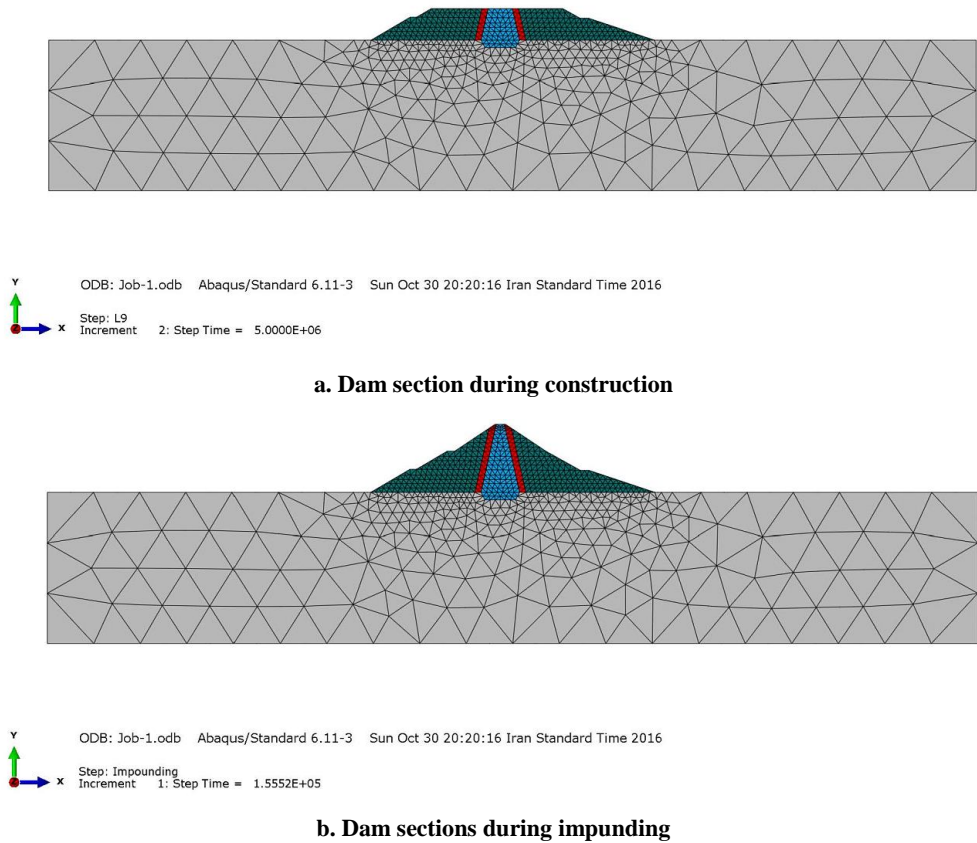


Figure 8. Dam sections during modeling

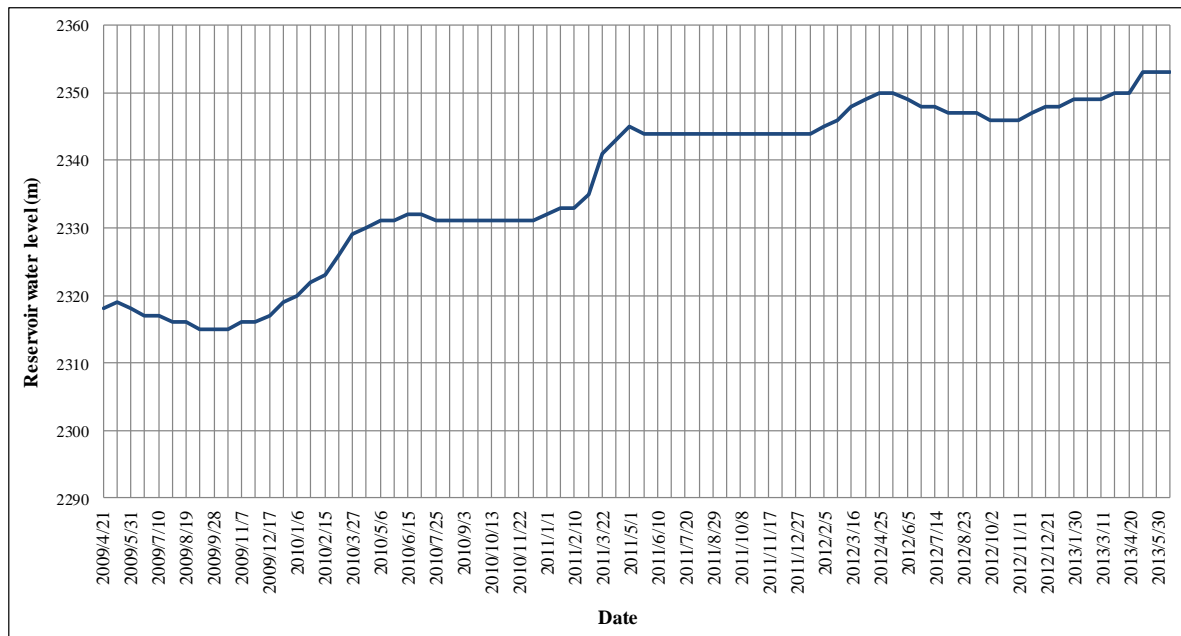


Figure 9. Changes in the dam reservoir water level

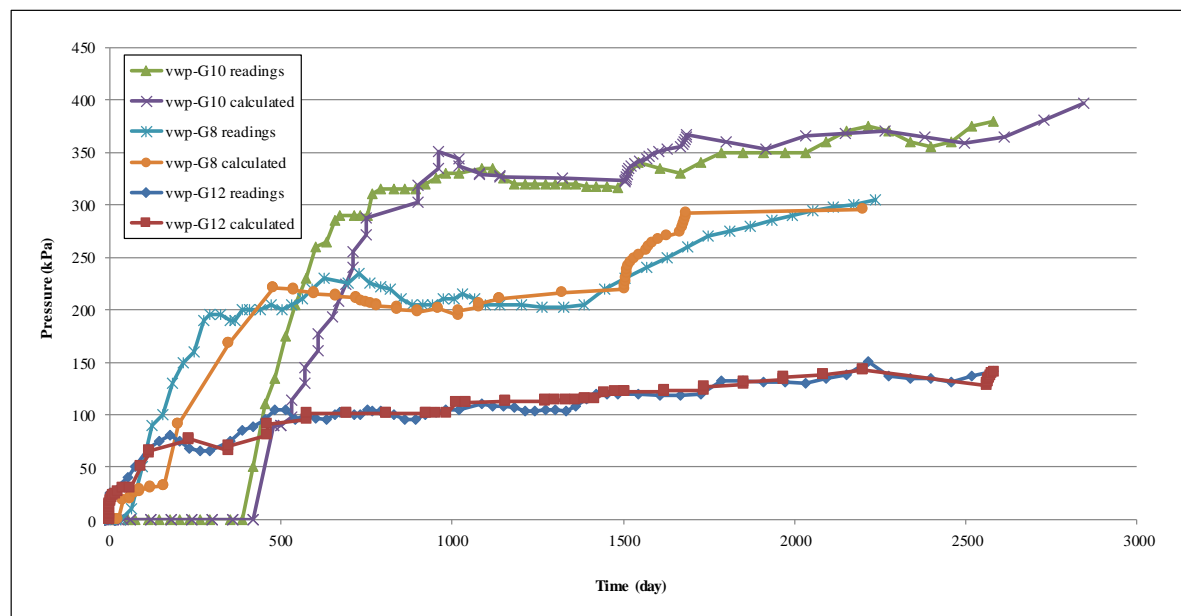


Figure 10. Comparison of water pressure from actual readings and finite elements modeling

Table 2. Permeability change interval in different parts of the dam body

Region	Foundation	Core	Filters	Shell
Upper limit (m/s)	5×10^{-7}	5×10^{-8}	1×10^{-4}	1×10^{-2}
Lower limit(m/s)	1×10^{-8}	1×10^{-9}	5×10^{-6}	5×10^{-4}

4.3. Defining the Objective Function

Regarding the Equation 1 it is clear that the time series related to the measurement of hydraulic heads and the flow discharge rates are required to create the objective function. Therefore, hydraulic head time series of the points in the finite elements model corresponding to the actual location of four piezometers G7, G8, G10 and G12, as shown in Figure 7, have been used as well as the total flow discharge rate time series of the model.

In this way, initially, a special permeability combination has been selected as the target combination of the problem and the hydraulic head time series in the mentioned piezometers and flow discharge rates associated with this particular state have been obtained. Table 4 shows the permeability coefficients in three target combinations in the present study.

Therefore, the purpose of inverse analysis is to identify these specified permeability combinations according to the values of hydraulic heads in the location of G7, G8, G10, and G12 piezometers and the flow discharge rates of the dam. In other words, it is assumed that the time series of the responses are obtained from the readings of the piezometers and flowmeters over the time, and just by having them the permeability coefficients in different parts of the dam are aimed to be identified and compared with the values considered in the design. Therefore, having the responses values, through each finite elements analysis the time series of the hydraulic heads and the total flow discharge rates and consequently the value of the objective function (the value of f in Equation 1) could be obtained for each combination. Obviously, in the ideal case, the value of the objective function would be zero.

Table 3. Factors and levels used in orthogonal design selection (in terms of m/s)

Level	Foundation beneath the dam to 10 meters depth	Foundation in depth between 10 and 20 meters	Foundation below 20 meter depth	Core	Filters	Shell
1	1×10^{-8}	1×10^{-8}	1×10^{-8}	1×10^{-9}	5×10^{-6}	5×10^{-4}
2	2×10^{-8}	2×10^{-8}	2×10^{-8}	2×10^{-9}	1×10^{-5}	1×10^{-3}
3	4×10^{-8}	4×10^{-8}	4×10^{-8}	4×10^{-9}	2×10^{-5}	2×10^{-3}
4	8×10^{-8}	8×10^{-8}	8×10^{-8}	8×10^{-9}	4×10^{-5}	4×10^{-3}
5	1.6×10^{-7}	1.6×10^{-7}	1.6×10^{-7}	1.6×10^{-8}	6×10^{-5}	6×10^{-3}
6	3.2×10^{-7}	3.2×10^{-7}	3.2×10^{-7}	3.2×10^{-8}	8×10^{-5}	8×10^{-3}
7	5×10^{-7}	5×10^{-7}	5×10^{-7}	5×10^{-8}	1×10^{-4}	1×10^{-2}

Table 4. Intended permeability values (m/s)

Region	Foundation beneath the dam to 10 meters depth	Foundation in depth between 10 and 20 meters	Foundation below 20 meter depth	Core	Filters	Shell
Case 1	5×10^{-8}	2×10^{-7}	5×10^{-8}	6×10^{-8}	2×10^{-5}	5×10^{-3}
Case 2	3×10^{-8}	1×10^{-8}	1×10^{-7}	4×10^{-8}	8×10^{-5}	1×10^{-4}
Case 3	5×10^{-7}	1×10^{-8}	5×10^{-7}	5×10^{-8}	5×10^{-5}	1×10^{-2}

4.4. Inverse Analysis

In order to perform the inverse analysis, the value of the objective function must be minimized. Thus, first, an artificial neural network has been constructed that has been used to give the values of the hydraulic heads, as well as the total flow discharge rate for any arbitrary combination at any time. In order to train the mentioned neural network, the answers obtained from 49 times of finite elements analysis of the dam model with different permeability combinations, derived from orthogonal design, have been used. The total number of available data was 7058 related to different times, of which 10% has been used for testing, 5% for validation, and the remainder for the training of the network. To determine the number of layers and the number of neurons in each layer, a large number of neural networks have been constructed, trained, tested and validated. Consequently, a back propagation neural network with a 4 internal layers of respectively 8, 35, 15, 5 neurons, had shown the best performance. Figure 12 shows the performance of this neural network during its raining, testing, and validating. As shown in this figure, the mean squared error of differences between actual results and the results obtained from the neural network is used to evaluate its performance.

Finally, the PSO algorithm has been used to minimize the objective function, where after so many times of trial and error the initial population of 100 individuals with 1000 steps, has shown the best end results. Figure 13 shows its performance in different steps and the final answers which have been obtained after 1000 generations are displayed in Table 6.

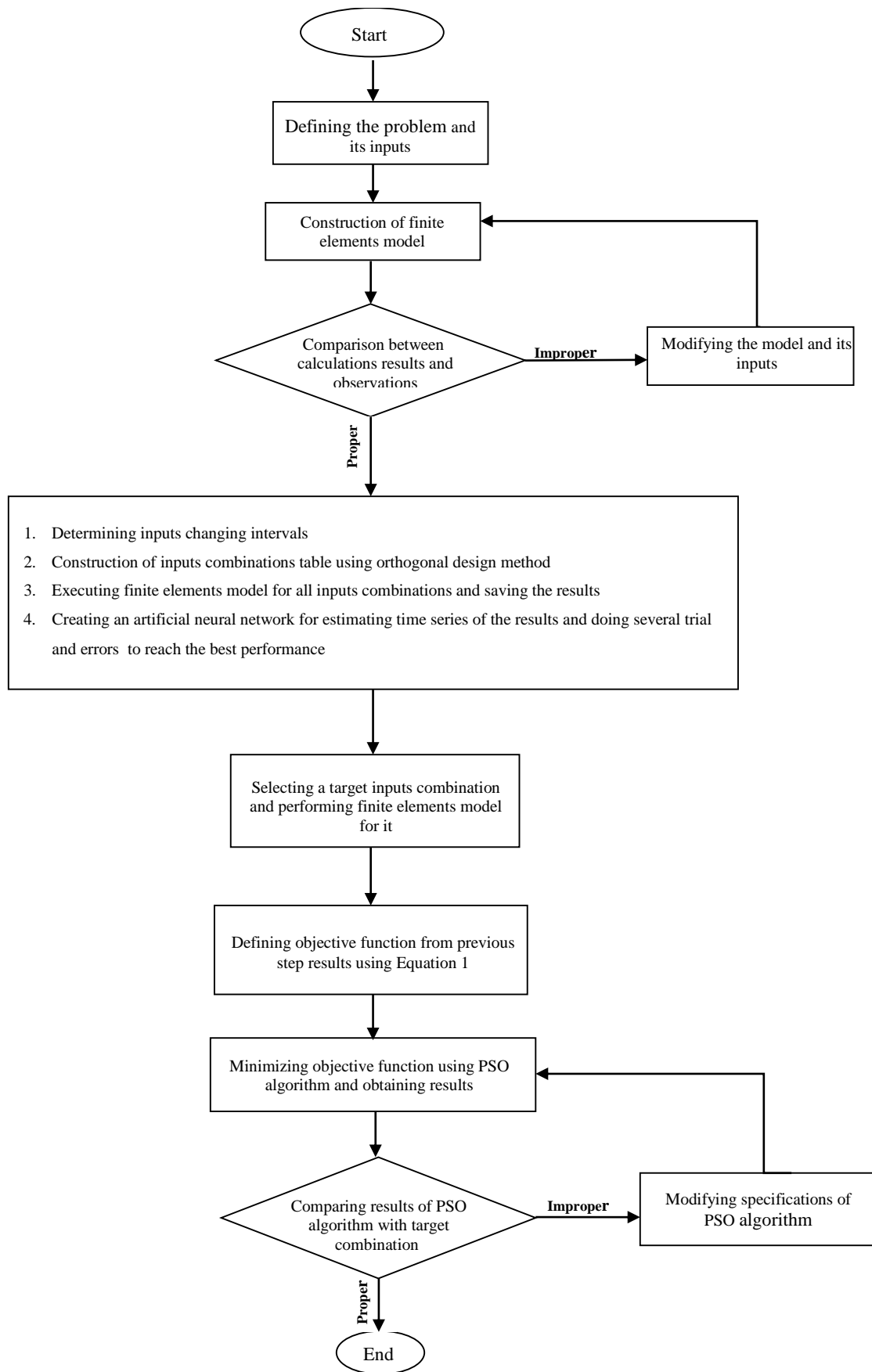


Figure 11. General flowchart of the proposed method

Table 6. Identified Permeability coefficients from inverse modeling (m/s)

Region	Foundation beneath the dam to 10 m depth	Foundation in depth between 10 and 20 m	Foundation below 20 m depth	Core	Filters	Shell
Case 1	5.0000×10^{-8}	2.0000×10^{-7}	5.0000×10^{-8}	6.0000×10^{-8}	2.0000×10^{-5}	5.0000×10^{-3}
Case 2	3.0000×10^{-8}	9.9969×10^{-9}	9.9999×10^{-8}	4.0000×10^{-8}	8.0003×10^{-5}	1.0021×10^{-4}
Case 3	5.0000×10^{-7}	9.9896×10^{-9}	4.9999×10^{-7}	5.0000×10^{-8}	5.0009×10^{-5}	1.0000×10^{-2}

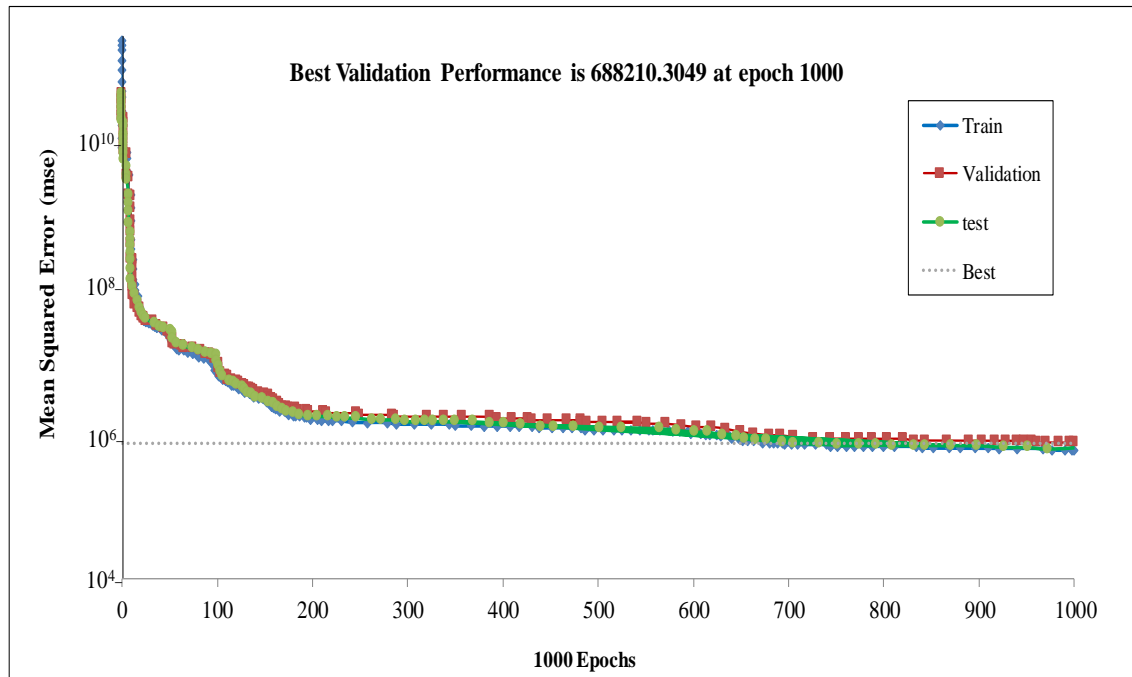


Figure 12. Performance of artificial neural network during training, testing and validation

5. Results and Discussions

In this research, an inverse analysis method was proposed to find the flow characteristics of a dam (especially the permeability of its different parts), taking into account the transient flow state and using the time series of hydraulic head changes and flow rate in the construction of the objective function. To investigate the efficiency of the proposed method in solving real large scaled problems, the inverse analysis method was used to estimate permeability coefficients in different parts of the Baft earth dam for three different permeability combinations.

As shown in Tables 4 and 6, in the case 1 the values of permeability coefficients obtained from the proposed method absolutely matched the target ones. In case 2 and 3 a small differences between target values and identified ones which are completely negligible, are seen. Also it is clear that the obtained results are not dependent on the amount of permeability values because in all parts of the dam whether in the core or foundation regions with very low permeability values or in the filters and shell regions with relatively greater hydraulic conductivities, identified values are completely reliable.

For a clearer understanding, Figure 14 provides bar charts to compare the target permeability values and the identified values from the proposed inverse analysis method for the three cases. The highest incompatibilities occurred in the foundation region in depth between 10 and 20 meters.

Application of a back propagation neural network substantially reduced the time needed for back analyses although it adds some errors to the answers. Because of facing with a large scale problem each time of ABAQUS modeling for an arbitrary composition takes at least 20 minutes. It means using direct PSO algorithm on the model was not applicable (100 individuals in each step) while using the neural network model made it possible. Acceptable performance of the applied neural network is clear from Figure 12.

As shown in Figure 13, in all three cases the global best values showed a smoothly reduction during iterations although the convergence speed in case one is much greater.

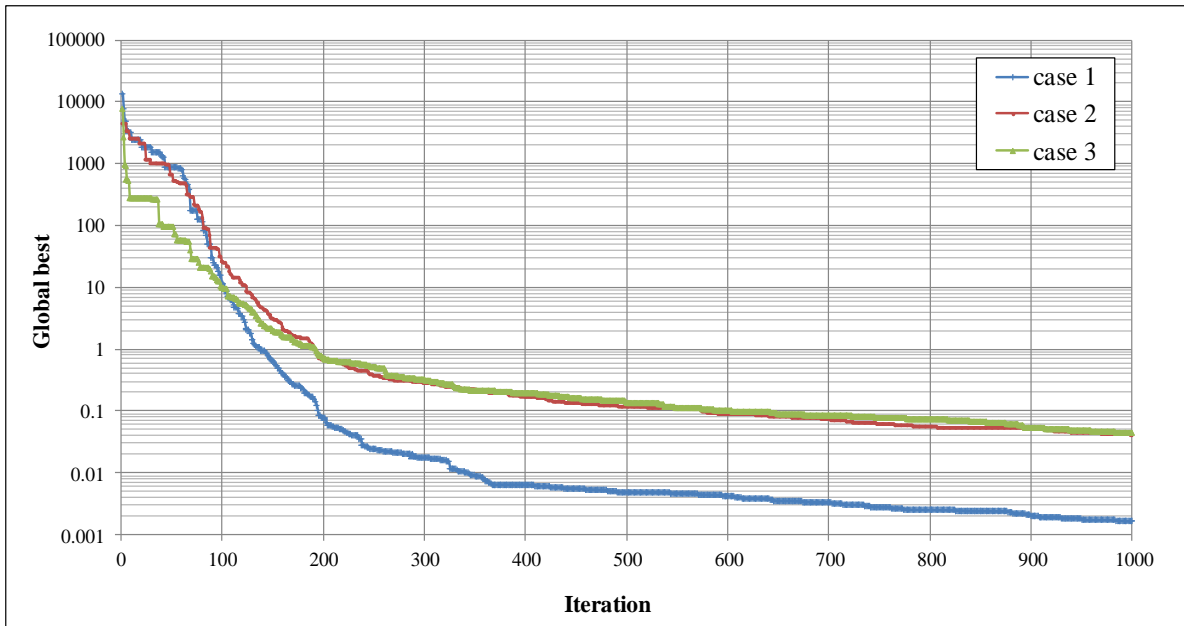
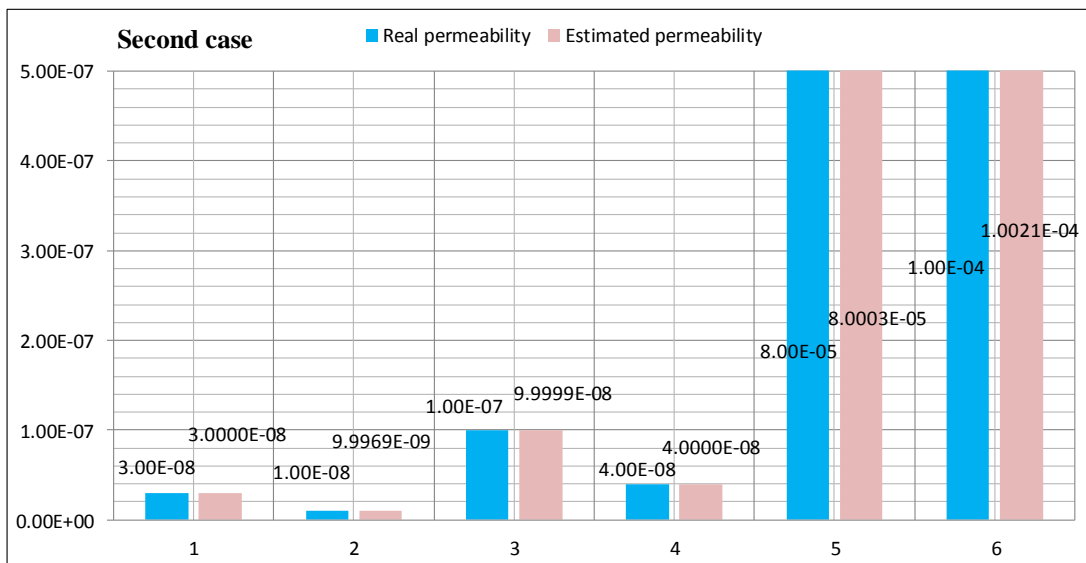
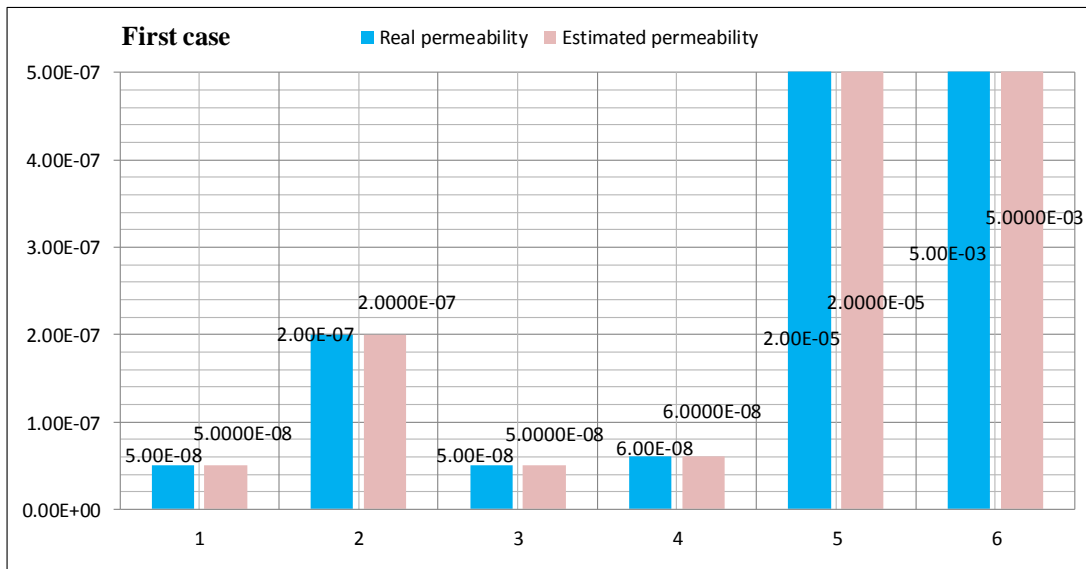


Figure 13. PSO algorithm performance



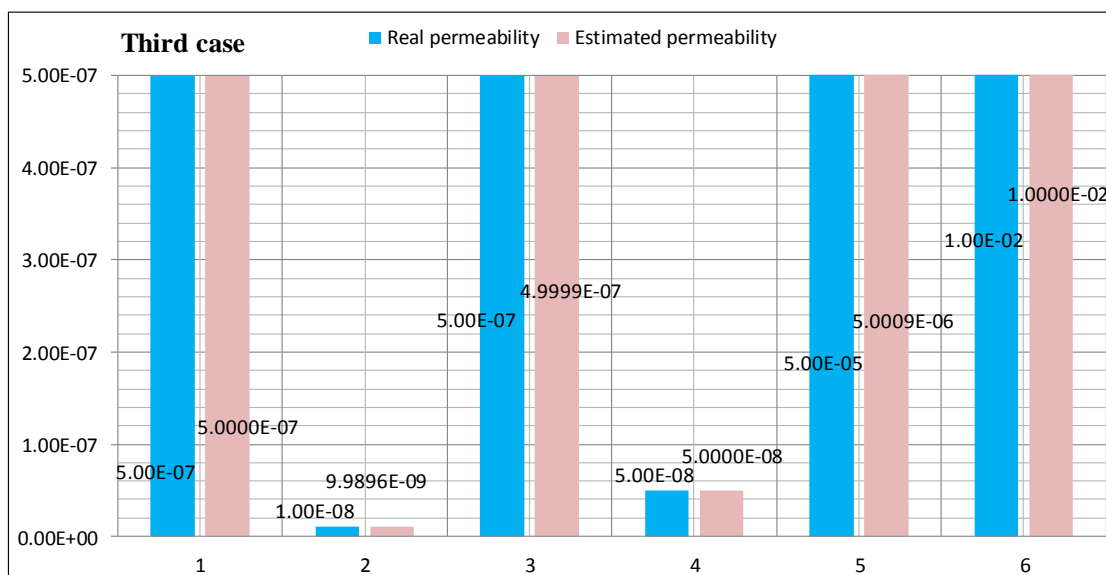


Figure 14. Comparison of identified and actual permeability coefficients

6. Conclusion

The proposed method is based on the use of finite element analysis and combination of the orthogonal designs, artificial neural networks and PSO optimization algorithms that significantly reduce the volume of computations and increase the speed of solving large-scale real-world problems in engineering.

Using proposed objective function led to a meaningful increase in the stability and accuracy of the inverse problem results. In addition the problem of ill-posedness has been fixed because the instability of the inverse solution stems from the fact that small errors in heads will cause serious errors in the identified permeability values. Furthermore, the anisotropic state could be considered in the same way if necessary.

The obtained results indicate the applicability of using the proposed method in locating unconventional leakage in geo-hydraulic problems and assessing the weakness of sealing system. Certainly, in order to improve accuracy and to find the location of the fault more precisely, it is possible to increase the number of divisions in modeling and have more accurate evaluation for the treatment operations.

Although the present research shows the ability of the proposed method to perform an inverse analysis, some imperfections such as ignoring the variability nature of parameters, the effect of embankments and excavations on the permeability of the bed layers, as well as the effect of climate change on effective parameters should be referred to, which are not considered in modeling to simplify the problem, and which can be used to conduct more accurate studies in future.

7. Conflicts of Interest

The authors declare no conflict of interest.

8. References

- [1] Ghamisi, Pedram, Micael S. Couceiro, Fernando M. L. Martins, and Jon Atli Benediktsson. "Multilevel Image Segmentation Based on Fractional-Order Darwinian Particle Swarm Optimization." *IEEE Transactions on Geoscience and Remote Sensing* 52, no. 5 (May 2014): 2382–2394. doi:10.1109/tgrs.2013.2260552.
- [2] Chang, Wei-Der, Jun-Ping Cheng, Ming-Chieh Hsu, and Liang-Chan Tsai. "Parameter Identification of Nonlinear Systems Using a Particle Swarm Optimization Approach." *2012 Third International Conference on Networking and Computing* (December 2012). doi:10.1109/icnc.2012.24.
- [3] Durmuş, B., and A. Gün. "Parameter identification using particle swarm optimization." In *Proceedings, 6th International Advanced Technologies Symposium, (IATS 11), Elazığ, Turkey, (2011): 188-192.*
- [4] Fernández Martínez, Juan L., Esperanza García Gonzalo, José P. Fernández Álvarez, Heidi A. Kuzma, and César O. Menéndez Pérez. "PSO: A Powerful Algorithm to Solve Geophysical Inverse Problems." *Journal of Applied Geophysics* 71, no. 1 (May 2010): 13–25. doi:10.1016/j.jappgeo.2010.02.001.

- [5] Poli, Riccardo. "Analysis of the Publications on the Applications of Particle Swarm Optimisation." *Journal of Artificial Evolution and Applications* (2008): 1–10. doi:10.1155/2008/685175.
- [6] Xiang, Yan, Shu-yan Fu, Kai Zhu, Hui Yuan, and Zhi-yuan Fang. "Seepage Safety Monitoring Model for an Earth Rock Dam Under Influence of High-Impact Typhoons Based on Particle Swarm Optimization Algorithm." *Water Science and Engineering* 10, no. 1 (January 2017): 70–77. doi:10.1016/j.wse.2017.03.005.
- [7] Chi, Shichun, Shasha Ni, and Zhenping Liu. "Back Analysis of the Permeability Coefficient of a High Core Rockfill Dam Based on a RBF Neural Network Optimized Using the PSO Algorithm." *Mathematical Problems in Engineering* 2015 (2015): 1–15. doi:10.1155/2015/124042.
- [8] Gamse, Sonja, and Michael Oberguggenberger. "Assessment of Long-Term Coordinate Time Series Using Hydrostatic-Season-Time Model for Rock-Fill Embankment Dam." *Structural Control and Health Monitoring* 24, no. 1 (April 6, 2016): e1859. doi:10.1002/stc.1859.
- [9] Chen, Yifeng, Chuangbing Zhou, and Yongqing Sheng. "Formulation of Strain-Dependent Hydraulic Conductivity for a Fractured Rock Mass." *International Journal of Rock Mechanics and Mining Sciences* 44, no. 7 (October 2007): 981–996. doi:10.1016/j.ijrmmms.2006.12.004.
- [10] Hamm, Se-Yeong, MoonSu Kim, Jae-Yeol Cheong, Jung-Yul Kim, Moon Son, and Tae-Won Kim. "Relationship Between Hydraulic Conductivity and Fracture Properties Estimated from Packer Tests and Borehole Data in a Fractured Granite." *Engineering Geology* 92, no. 1–2 (June 2007): 73–87. doi:10.1016/j.enggeo.2007.03.010.
- [11] Manda, Alex K., Stephen B. Mabee, David F. Boutt, and Michele L. Cooke. "A Method of Estimating Bulk Potential Permeability in Fractured-Rock Aquifers Using Field-Derived Fracture Data and Type Curves." *Hydrogeology Journal* 21, no. 2 (November 10, 2012): 357–369. doi:10.1007/s10040-012-0919-2.
- [12] Ren, Jie, Zhen-zhong Shen, Jie Yang, and Chong-zhen Yu. "Back Analysis of the 3D Seepage Problem and Its Engineering Applications." *Environmental Earth Sciences* 75, no. 2 (January 2016). doi:10.1007/s12665-015-4837-1.
- [13] Turkmen, Sedat. "Treatment of the Seepage Problems at the Kalecik Dam (Turkey)." *Engineering Geology* 68, no. 3–4 (March 2003): 159–169. doi:10.1016/s0013-7952(02)00225-9.
- [14] Jiang, Zhenxiang, and Jinping He. "Detection Model for Seepage Behavior of Earth Dams Based on Data Mining." *Mathematical Problems in Engineering* 2018 (2018): 1–11. doi:10.1155/2018/8191802.
- [15] Zhang, Jiafa, Jinlong Wang, and Haodong Cui. "Causes of the Abnormal Seepage Field in a Dam with Asphaltic Concrete Core." *Journal of Earth Science* 27, no. 1 (February 2016): 74–82. doi:10.1007/s12583-016-0623-6.
- [16] Tarantola, Albert. "Inverse Problem Theory and Methods for Model Parameter Estimation" (January 2005). doi:10.1137/1.9780898717921.
- [17] Lingireddy, Srinivasa. "Aquifer Parameter Estimation Using Genetic Algorithms and Neural Networks." *Civil Engineering and Environmental Systems* 15, no. 2 (March 1998): 125–144. doi:10.1080/02630259808970234.
- [18] Yeh, William W-G. "Review of Parameter Identification Procedures in Groundwater Hydrology: The Inverse Problem." *Water Resources Research* 22, no. 2 (February 1986): 95–108. doi:10.1029/wr022i002p00095.
- [19] Alcolea, Andrés, Jesús Carrera, and Agustín Medina. "Pilot Points Method Incorporating Prior Information for Solving the Groundwater Flow Inverse Problem." *Advances in Water Resources* 29, no. 11 (November 2006): 1678–1689. doi:10.1016/j.advwatres.2005.12.009.
- [20] Bastani, Mehrdad, Majid Kholghi, and Gholam Reza Rakhshandehroo. "Inverse Modeling of Variable-Density Groundwater Flow in a Semi-Arid Area in Iran Using a Genetic Algorithm." *Hydrogeology Journal* 18, no. 5 (March 30, 2010): 1191–1203. doi:10.1007/s10040-010-0599-8.
- [21] Karpouzou, D. K., F. Delay, K. L. Katsifarakis, and G. de Marsily. "A Multipopulation Genetic Algorithm to Solve the Inverse Problem in Hydrogeology." *Water Resources Research* 37, no. 9 (September 2001): 2291–2302. doi:10.1029/2000wr900411.
- [22] Samuel, Manoj P., and Madan K. Jha. "Estimation of aquifer parameters from pumping test data by genetic algorithm optimization technique." *Journal of irrigation and drainage engineering* 129, no. 5 (2003): 348–359. doi:10.1061/(asce)0733-9437(2003)129:5(348).
- [23] Dietrich, C R, and G N Newsam. "Sufficient Conditions for Identifying Transmissivity in a Confined Aquifer." *Inverse Problems* 6, no. 3 (June 1, 1990): L21–L28. doi:10.1088/0266-5611/6/3/002.
- [24] Jing, L. H., S. C. Duan, and S. Q. Yang. "Application of seepage back analysis to engineering design." *Chinese Journal of Rock Mechanics and Engineering* 26 (2007): 4503–4509.

- [25] Chang, Ya-Chi, Hund-Der Yeh, and Yen-Chen Huang. "Determination of the Parameter Pattern and Values for a One-Dimensional Multi-Zone Unconfined Aquifer." *Hydrogeology Journal* 16, no. 2 (October 19, 2007): 205–214. doi:10.1007/s10040-007-0228-3.
- [26] Garcia, Luis A., and Abdalla Shigidi. "Using Neural Networks for Parameter Estimation in Ground Water." *Journal of Hydrology* 318, no. 1–4 (March 2006): 215–231. doi:10.1016/j.jhydrol.2005.05.028.
- [27] Virbulis, Janis, Uldis Bethers, Tomas Saks, Juris Sennikovs, and Andrejs Timuhins. "Hydrogeological Model of the Baltic Artesian Basin." *Hydrogeology Journal* 21, no. 4 (March 26, 2013): 845–862. doi:10.1007/s10040-013-0970-7.
- [28] Woodbury, Allan D., and Tadeusz J. Ulrych. "A Full-Bayesian Approach to the Groundwater Inverse Problem for Steady State Flow." *Water Resources Research* 36, no. 8 (August 2000): 2081–2093. doi:10.1029/2000wr900086.
- [29] Dai, Zhenxue, Elizabeth Keating, Carl Gable, Daniel Levitt, Jeff Heikoop, and Ardyth Simmons. "Stepwise Inversion of a Groundwater Flow Model with Multi-Scale Observation Data." *Hydrogeology Journal* 18, no. 3 (November 10, 2009): 607–624. doi:10.1007/s10040-009-0543-y.
- [30] Gong, Wenyin, Zihua Cai, and Liangxiao Jiang. "Enhancing the Performance of Differential Evolution Using Orthogonal Design Method." *Applied Mathematics and Computation* 206, no. 1 (December 2008): 56–69. doi:10.1016/j.amc.2008.08.053.
- [31] Coppola Jr, Emery, Ferenc Szidarovszky, Mary Poulton, and Emmanuel Charles. "Artificial neural network approach for predicting transient water levels in a multilayered groundwater system under variable state, pumping, and climate conditions." *Journal of Hydrologic Engineering* 8, no. 6 (2003): 348–360. doi:10.1061/(asce)1084-0699(2003)8:6(348).
- [32] Neaupane, K. "Use of Backpropagation Neural Network for Landslide Monitoring: a Case Study in the Higher Himalaya." *Engineering Geology* (May 2004): 213–226. doi:10.1016/s0013-7952(04)00080-8.
- [33] Kurtulus, Bedri, and Moumtaz Razack. "Evaluation of the Ability of an Artificial Neural Network Model to Simulate the Input-Output Responses of a Large Karstic Aquifer: The La Rochefoucauld Aquifer (Charente, France)." *Hydrogeology Journal* 15, no. 2 (September 23, 2006): 241–254. doi:10.1007/s10040-006-0077-5.
- [34] Rafiai, H., A. Jafari, and A. Mahmoudi. "Application of ANN-Based Failure Criteria to Rocks under Polyaxial Stress Conditions." *International Journal of Rock Mechanics and Mining Sciences* 59 (April 2013): 42–49. doi:10.1016/j.ijrmmms.2012.12.003.
- [35] Ko, Nak-Youl, Sung-Hoon Ji, Yong-Kwon Koh, and Jong-Won Choi. "Consideration of Boreholes in Modeling of the Regional-Scale Groundwater Flow in a Fractured Rock." *Engineering Geology* 149–150 (November 2012): 13–21. doi:10.1016/j.enggeo.2012.08.008.